Instability in Molecular Beam Epitaxy due to Fast Edge Diffusion and Corner Diffusion Barriers

M. V. Ramana Murty* and B. H. Cooper

Department of Physics and Cornell Center for Materials Research, Cornell University, Ithaca, New York 14853

(Received 10 August 1998; revised manuscript received 23 December 1998)

Fast edge diffusion leads to a diffusion bias during molecular beam epitaxy. Kinetic Monte Carlo simulations on a solid-on-solid model incorporating fast edge diffusion clearly show pattern formation. Fast edge diffusion combined with an excess barrier to go past the outer corner of an island results in wavy steps, similar to the Bales-Zangwill instability, in the step flow growth regime. The evolution of surface morphology with fast edge diffusion and corner diffusion barriers is discussed in terms of the surface diffusion current.

PACS numbers: 68.35.Fx, 68.35.Bs, 68.55.–a, 81.15.Hi

During molecular beam epitaxy (MBE), atoms arrive at the surface uncorrelated in space and time. The resulting surface morphology is determined by the activation barriers for the different motions of atoms on the terraces and along and over step edges. A long standing problem is how the activation barriers for atomic moves influence surface morphology, often discussed in terms of the height-height correlation, step density and directions, and interface width. Developing such an understanding can suggest new ways to manipulate the deposition conditions to achieve the desired surface morphology, which could be, for example, a smooth surface or a regular arrangement of mounds and pits.

Recently it has been shown that a diffusion bias in the uphill direction plays a key role in pattern formation, leading to an approximately regular arrangement of mounds and pits [1–3]. Similar patterns have also been observed after sputtering of metal and semiconductor surfaces with 0.1–1 keV noble gas ions [4,5]. Sources of diffusion bias that have been discussed previously involve *adatom motion on the terrace*, and include an Ehrlich-Schwoebel (ES) barrier for interlayer diffusion and an adatom-step attraction [1,6]. Such step edge barriers have been found experimentally [7] and in first principles calculations [8] in a number of growth systems. Pattern formation is often taken to indicate the existence of a diffusion bias for atom motion on the terrace. Less attention has been paid to the role of diffusion along step edges in the evolution of three-dimensional surface morphology. Diffusion barriers to go past outside corners of islands have been shown to influence the shapes of two-dimensional islands in submonolayer epitaxy [9] and the directions of step edges in mounds and pits [10,11].

In this Letter, we show that pattern formation can result from *atom motion along step edges*, even in the *absence* of repulsive ES or attractive step edge barriers for atom motion on the terrace. Fast edge diffusion leads to a diffusion bias during MBE since atom motion along step edges is directed towards inner corner sites as islands try to become compact. Kinetic Monte Carlo (KMC) simulations on a solid-on-solid (SOS) model incorporating fast edge diffusion clearly show pattern formation. In addition, the presence of an excess barrier to go past the outer corner of an island during edge diffusion results in wavy steps, similar to the Bales-Zangwill instability [12], in the step flow growth regime.

The KMC simulations were performed on a SOS model with a simple cubic lattice. Periodic boundary conditions were used in the transverse directions. The energy of an atom with n lateral nearest-neighbor bonds is $-n\varepsilon$. We consider two models for the activation barriers. In the first model (model A), the jump frequency f depends on the energies E_i and E_j of the atom in the initial (i) and final (j) states and a parameter ε_d according to

$$f = \begin{cases} \nu \exp[-(E_j - E_i + \varepsilon_d)/k_B T], & E_i < E_j, \\ \nu \exp[-\varepsilon_d/k_B T], & E_i \geq E_j, \end{cases} \quad (1)$$

Here ν is the attempt frequency, assumed to be the same for all jumps, and k_B and T are the Boltzmann constant and the substrate temperature, respectively. In this model atom diffusion along the edges of $\langle 100 \rangle$ steps is as fast as adatom diffusion on the terrace. However, diffusion past the inside and outside corners of islands is slow since it requires detachment (bond breaking). In the second model (model B), the jump frequency depends on the energy in the initial state according to

$$f = \nu \exp[-(\varepsilon_d - E_i)/k_B T]. \quad (2)$$

In model B, the activation barrier for atom diffusion along $\langle 100 \rangle$ steps is higher than the adatom diffusion barrier on the terrace. In both models A and B, only nearest neighbor jumps are permitted. The parameter values are $\varepsilon = 0.3$ eV, $\varepsilon_d = 0.3$ eV, and $\nu = 10^{12}$ s^{-1}. The deposition rate is 1 monolayer (ML) per sec. We will also discuss a model A′ that is the same as model A except that, in addition, next-nearest-neighbor jumps around the outside corner of step edges are permitted. (Such corner jumps are, however, not permitted in dimers and trimers in model A′.) Downward funneling [13] is not included in order to show the effect of edge diffusion more clearly. We note that all models discussed in this paper obey

 0031-9007/99/83(2)/352(4)$15.00

detailed balance and that there is no repulsive or attractive step edge barrier for adatom motion on the terrace in models A, A′, and B.

Figure 1 shows snapshots of the surface after deposition of (a) 200 ML at 173 K with model A; (b) 4 ML at 373 K with model A; (c) 200 ML at 173 K with model B; and (d) 100 ML at 223 K with model B. Growth was initiated on the singular (001) surface in Figs. 1(a), 1(c), and 1(d) and on a vicinal surface with steps initially along the [100] direction and a terrace width of 10 lattice units in Fig. 1(b). The surface morphologies for the two models are dramatically different. On the singular surface, a pattern of mounds and pits with a characteristic lateral length scale is observed with model A [Fig. 1(a)]. The step edges along the mounds and pits are frequently along the ⟨110⟩ directions. On the vicinal surface, a kinetic instability in the form of wavy steps, similar to the Bales-Zangwill instability [12], is observed with model A [Fig. 1(b)]. In model B, the islands are dendritic and are arranged with no apparent pattern or periodicity [Figs. 1(c) and 1(d)].

The lateral correlations between features on the surface can be quantified in terms of the height-height correlation function $H(\mathbf{R})$

$$H(\mathbf{R}) = \frac{1}{N} \sum_{S} h(\mathbf{r}) h(\mathbf{r} + \mathbf{R}) . \qquad (3)$$

Here, $h(\mathbf{r})$ is the height at the position $\mathbf{r}$ measured with respect to the average height and N is the total number of surface sites. The function $H(R)$ in Fig. 2 is the average for $\mathbf{R}$ along the [110] and [$\bar{1}$10] directions.

Figure 2(a) shows $H(R)$ at 173 K and different film thicknesses for model A. The oscillatory $H(R)$ indicates an approximately regular arrangement of features on the surface [14]. The rms roughness w is given by $\sqrt{H(0)}$ and the first zero crossing of $H(R)$ is a measure of the length scale l on the surface. For film thicknesses greater than 50 ML, the variation of w and l with time t was found to be consistent with a power law, $w \sim t^{0.37 \pm 0.03}$ and $l \sim t^{0.20 \pm 0.02}$. The very different scaling exponents for w and l (and the close-packed arrangement of mounds and pits) indicate that there is no slope selection along the sides of mounds and pits up to 500 ML. Figure 2(b) shows $H(R)$ at 173 K for model B. There are no (or very weak) oscillations in $H(R)$, indicating no regularity in the arrangement of features on the surface.

Determination of the surface diffusion current j_s can give insight into the microscopic mechanisms leading to the different surface morphologies. Since the current is expected to be a function of slope, $(10L)$ vicinal surfaces with steps initially running along the [010] direction were chosen as the starting surfaces. The current was determined by evaluating

$$j_s = \frac{p_+ - p_-}{N\theta} F , \qquad (4)$$

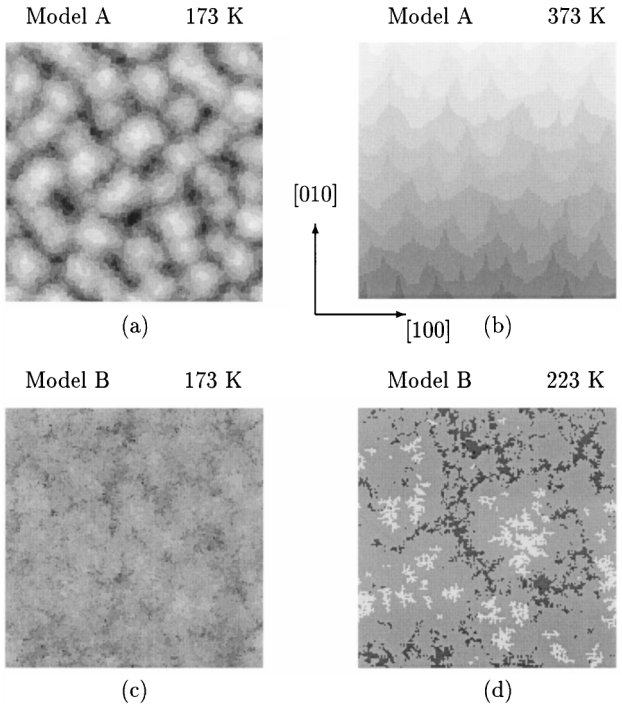

FIG. 1. Snapshots of the surface morphology after deposition of (a) 200 ML at 173 K, model A; (b) 4 ML at 373 K, model A; (c) 200 ML at 173 K, model B; and (d) 100 ML at 223 K, model B. The size of the simulation cell is 160 × 160 in (a), (c), and (d), and 100 × 400 lattice units in (b). Note that the scale is 1:4 for [100] and [010] directions in (b). The grey scale is used to indicate height with lighter areas representing higher points.

where θ is the total number of atoms deposited in ML, F is the deposition flux (1 ML/s), and p_+ and p_- are the total number of hops, counted during deposition, up to the coverage θ in the [100] (uphill) and [$\bar{1}$00] (downhill) directions, respectively [15,16]. Figure 3(a) shows j_s as a function of slope $m = L^{-1}$ with $\theta = 0.10$ ML for models A and B. A finite diffusion current is present in model A. No current was found in model B within the error of the calculation. Figure 3(b) shows the contribution to j_s from atoms diffusing on the terrace (coordination 0) and along the edges of steps (coordination 1) for model A. The current was determined up to different

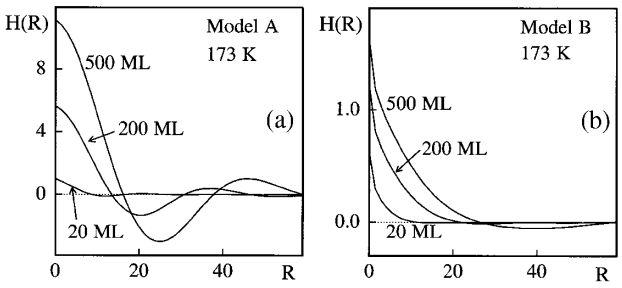

FIG. 2. The height-height correlation function $H(R)$ from the surfaces at different film thicknesses for (a) model A and (b) model B. The data are averaged over 40 simulations.

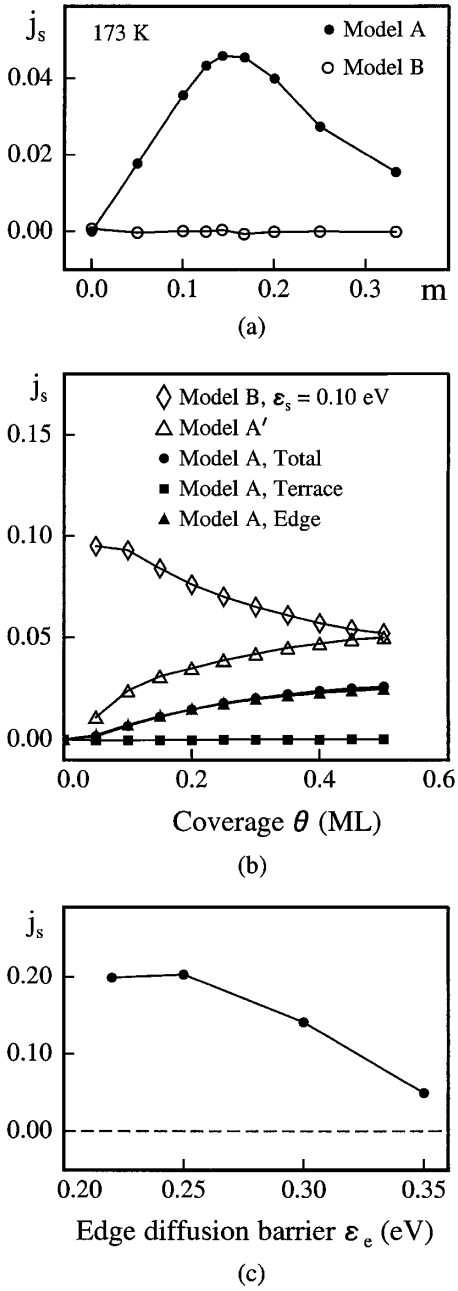

FIG. 3. (a) Surface diffusion current j_s on vicinal surfaces of slope m for models A and B. The current j_s was calculated according to Eq. (4) up to $\theta = 0.10$ ML at 173 K. (b) Total surface diffusion current and the terrace and edge diffusion components as a function of coverage θ on a vicinal surface with $m = 0.02$ for model A. Also shown is the total j_s for model A′ and a modified model B with an ES barrier of $\varepsilon_s = 0.10$ eV. (c) Total current j_s for model A′ modified to have an edge diffusion barrier ε_e and no corner barrier. The terrace size was $L = 10$ and $\theta = 0.10$ ML.

coverages θ on a vicinal surface of slope $m = 0.02$. For model A, atoms diffusing on the terrace do not face any diffusion bias, and almost all j_s arises from atoms diffusing along the step edges. Figure 3(b) also shows j_s for model A′ and model B modified to include an ES barrier $\varepsilon_s = 0.10$ eV. Terrace diffusion gives rise to the diffusion bias in model B with $\varepsilon_s = 0.10$ eV, and the edge diffusion is the source of diffusion bias in model A′. We also show results from model A′ modified to have an edge diffusion barrier ε_e; Fig. 3(c) shows j_s as a function of ε_e with $\theta = 0.10$ ML and $L = 10$. The diffusion bias persists even as the edge diffusion gets faster.

We now discuss how edge diffusion gives rise to a diffusion current during deposition on a vicinal surface. Figure 4 shows a step edge and the activation barriers in models A and B for a sequence of moves along the step edge. For model A, the activation barrier for diffusion along the step edge is ε_d except near the corners. Near the outside corner, at position X, an atom is more likely to hop to position W than to position Y. On the other hand, an atom at position V faces a relatively large activation barrier to move to the neighboring positions U and W. Thus, position X acts as a reflecting site and position V acts as an absorbing site for atoms moving along the step edge. As shown in Fig. 3(b), the diffusion current is presented even in model A′, where X does not act as a reflecting site. The diffusion current arises when an island becomes compact by drawing atoms moving along the step edge to sites such as V. Beginning with straight step edges in model A, j_s increases from zero with coverage [Fig. 3(b)] due to the increase in roughness of the steps (by symmetry, islands nucleated on the terrace do not contribute to j_s in Fig. 3). In model B, the slow diffusion of atoms with coordination 1 (at 173 and 223 K) results in a vanishing (or very small) j_s.

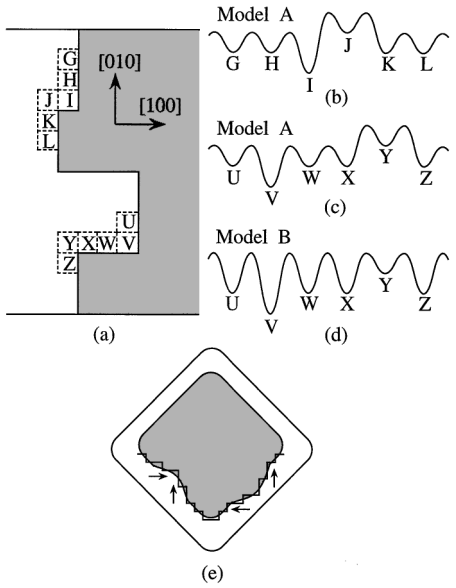

FIG. 4. (a) Schematic of a vicinal surface with a rough step edge. The energy contours for an atom diffusing along the step edge are shown for (b) path G-L, model A; (c) path U-Z, model A; and (d) path U-Z, model B. (e) Perturbations from the ⟨110⟩ step direction result in diffusion currents indicated by the arrows for model A. The shaded areas in (a) and (e) represent the upper terrace.

We now describe the evolution of surface morphology in model A during growth, starting with the singular (001) surface [Fig. 1(a)]. Growth begins by the nucleation of islands at submonolayer coverages. Most atoms that land within a distance of the order of the diffusion length of an island join the island instead of nucleating a new island. Islands in the second layer will nucleate preferentially away from step edges, i.e., where the adatom concentration is the highest [17]. Model A shows an earlier onset of second layer nucleation compared to model B, possibly associated with a change from a dendritic (model B) to a more compact (model A) island shape [18]. The preferred $\langle 110 \rangle$ step directions in the mounds and pits arise as follows. Consider an atom approaching the kink site I along a step edge (Fig. 4). An atom at position H has equal probabilities of hopping to sites G and I. However, an atom at position K is more likely to jump to position L than position J. The corner diffusion barrier can thus be thought of as an ES barrier for atom diffusion along the edge of the step [10]. The $\langle 100 \rangle$ steps are unstable during epitaxy and the kink density on the $\langle 100 \rangle$ steps increases. The step directions change until the steps point along the $\langle 110 \rangle$ directions, where, by symmetry, the diffusion bias for atoms moving along the step edge vanishes. Deposition causes perturbations from the $\langle 110 \rangle$ step directions. The resulting diffusion current due to edge diffusion has an uphill component as indicated in Fig. 4(e). Continuum equations incorporating an uphill current show pattern formation (mounds and pits) with a characteristic lateral length scale [1,3,15,19]. The length scale on the surface increases as neighboring mounds (and pits) coalesce. In our simulations, there is no slope selection as there is no slope m for which $j_s = 0$ and $\partial j_s / \partial m < 0$ [3]. During step flow growth, [010] steps are unstable and become wavy as shown in Fig. 1(b).

How important is edge diffusion compared to the ES barrier as a source of diffusion bias? Calculations of the uphill current in the Fe/Fe(001), Ag/Ag(001), and Ge/Ge(001) systems using model parameters from the literature [14,20] indicate that the contribution of fast edge diffusion is comparable to that of the ES barrier. All of the above systems exhibit pattern formation [20,21].

In conclusion, KMC simulations show that fast edge diffusion leads to pattern formation in molecular beam epitaxy. In addition, wavy steps similar to those of the Bales-Zangwill instability, are observed in step flow growth when the barrier to go past the outer corner of an island exceeds the straight step barrier for atoms moving along a step edge. Uphill current induced by edge diffusion may be important in systems that exhibit quasi-layer-by-layer growth and compact two-dimensional islands.

We thank László Barabasi for suggesting the calculation of the surface diffusion current, Jim Sethna for a critical reading of the manuscript, and Chris Henley for useful discussions. This work made use of the CCMR facilities supported by NSF under Award No. DMR-9632275 and the resources of the Cornell Theory Center. Additional support was provided by AFOSR under Grant No. F49620-97-1-0020.

*Present address: Materials Science Division, Argonne National Laboratory, Argonne, IL 60439.
Email address: murty@anl.gov

[1] J. Villain, J. Phys. I (France) **1**, 19 (1991).
[2] H.-J. Ernst *et al.,* Phys. Rev. Lett. **72**, 112 (1994); M. Bott *et al.,* Surf. Sci. **272**, 161 (1992); J. E. van Nostrand *et al.,* Phys. Rev. Lett. **74**, 1127 (1995); J. A. Stroscio *et al.,* Phys. Rev. Lett. **75**, 4246 (1995); J.-K. Zuo and J. F. Wendelken, Phys. Rev. Lett. **78**, 2791 (1997).
[3] M. D. Johnnson *et al.,* Phys. Rev. Lett. **72**, 116 (1994).
[4] T. Michely and G. Comsa, Nucl. Instrum. Methods Phys. Res., Sect. B **82**, 207 (1993); M. Ritter *et al.,* Surf. Sci. **348**, 243 (1996); S. J. Chey *et al.,* Phys. Rev. B **52**, 16 696 (1995).
[5] M. V. R. Murty *et al.,* Phys. Rev. Lett. **80**, 4713 (1998).
[6] J. G. Amar and F. Family, Phys. Rev. Lett. **77**, 4584 (1996).
[7] G. Ehrlich and F. G. Hudda, J. Chem. Phys. **44**, 1039 (1966); S. C. Wang and G. Ehrlich, Phys. Rev. Lett. **70**, 41 (1993); K. Morgenstern *et al.,* Surf. Sci. **253**, 956 (1996).
[8] R. Stumpf and M. Scheffler, Phys. Rev. B **53**, 4958 (1996); P. J. Feibelman, Phys. Rev. Lett. **81**, 168 (1998).
[9] M. Hohage *et al.,* Phys. Rev. Lett. **76**, 2366 (1996); J. Jacobsen *et al.,* Phys. Rev. Lett. **74**, 2295 (1995); Z. Zhang *et al.,* Phys. Rev. Lett. **73**, 1829 (1994).
[10] M. Biehl *et al.,* Europhys. Lett. **41**, 443 (1998).
[11] After this work was submitted, we have learned about two papers discussing the role of edge diffusion in surface morphology evolution: O. Pierre-Louis *et al.,* Phys. Rev. Lett. **82**, 3661 (1999); J. Amar (to be published).
[12] G. S. Bales and A. Zangwill, Phys. Rev. B **41**, 5500 (1990).
[13] J. W. Evans *et al.,* Phys. Rev. B **41**, 5410 (1990).
[14] P. Hahn *et al.,* Appl. Phys. **51**, 2079 (1980); M. C. Bartelt and J. W. Evans, Phys. Rev. Lett. **75**, 4250 (1995).
[15] J. Krug *et al.,* Phys. Rev. Lett. **70**, 3271 (1993).
[16] A.-L. Barabasi and H. E. Stanley, *Fractal Concepts in Surface Growth* (Cambridge University Press, Cambridge, England, 1995), Chaps. 12–20; *ibid.*, Append. A.
[17] J. Tersoff *et al.,* Phys. Rev. Lett. **72**, 266 (1994).
[18] M. V. R. Murty and B. H. Cooper (to be published); A. L. Barabasi (private communication).
[19] M. Siegert and M. Plischke, Phys. Rev. Lett. **73**, 1517 (1994).
[20] J. A. Stroscio and D. T. Pierce, J. Vac. Sci. Technol. B **12**, 1783 (1993); J. G. Amar and F. Family, Phys. Rev. B **52**, 13 801 (1996); J. E. van Nostrand *et al.,* Phys. Rev. B **57**, 12 536 (1998); C.-M. Zhang *et al.,* Surf. Sci. **406**, 178 (1998).
[21] J. A. Stroscio *et al.,* Phys. Rev. Lett. **75**, 4246 (1995); J. E. van Nostrand *et al.,* Phys. Rev. Lett. **74**, 1127 (1995); W. C. Elliott *et al.,* Phys. Rev. B **54**, 17 938 (1996).